Journal of Photochemistry and Photobiology A: Chemistry 274 (2014) 27–32

Contents lists available at ScienceDirect

Journal of Photochemistry and Photobiology A: Chemistry

journal homepage: www.elsevier.com/locate/jphotochem

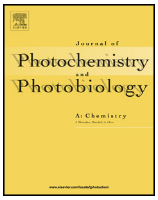

Photodegradation of 4,4-Bis(4-hydroxyphenyl)valeric acid and its inclusion complex with β-cyclodextrin in aqueous solution

Victoria A. Salomatova[a,*], Ivan P. Pozdnyakov[a,b], Vadim V. Yanshole[b,c], Feng Wu[d], Vjacheslav P. Grivin[a,b], Nikolay M. Bazhin[a], Victor F. Plyusnin[a,b]

[a] V.V. Voevodsky Institute of Chemical Kinetics and Combustion, 3 Institutskaya str., 630090 Novosibirsk, Russian Federation
[b] Novosibirsk State University, 2 Pirogova Str., 630090 Novosibirsk, Russian Federation
[c] International Tomography Center, 3a Institutskaya str., 630090 Novosibirsk, Russian Federation
[d] Department of Environmental Science, Wuhan University, 430072 Wuhan, Hubei, PR China

ARTICLE INFO

Article history:
Received 30 July 2013
Received in revised form
26 September 2013
Accepted 28 September 2013
Available online xxx

Keywords:
Flash photolysis
Kinetics
Bisphenol
Photoionization
Phenoxyl radical
β-Cyclodextrin

ABSTRACT

Nanosecond laser flash photolysis and time-resolved fluorescence were used to study photochemistry of 4,4-Bis(4-hydroxyphenyl)valeric acid (diphenolic acid, DPA) and complex of DPA with β-cyclodextrin (DPA-βCD) in aqueous solutions. For both systems the primary photochemical process was found to be photoionization with the formation of a hydrated electron–phenoxyl radical pair. Inclusion of DPA in cyclodextrin cavity leads to the great increase of photoionization and fluorescence quantum yield (from 0.01 to 0.14) as well as fluorescence lifetime (from 0.17 to 2.9 ns) due to decreasing of the quenching rate of the singlet excited state of complexed DPA by solvent molecules.

1. Introduction

4,4-Bis(4-hydroxyphenyl)valeric acid (DPA) is industrially important chemical, which is widely used in production of alkyd resin, phenol-formaldehyde resins, printing-inks, adhesives and coatings [1]. DPA is a close structural analog of widely known endocrine disruptor-bisphenol A and so DPA potentially can exhibit estrogenic activity and toxicity in environment [2,3]. During their production and consumption bisphenols spread and accumulate in environment causing damage to the living organisms [4,5]. Ordinary water treatment processes are not enough effective to removal of majority of synthetic estrogens and in some cases leads to formation of byproducts of unknown nature and toxicity [6]. These facts lead to prohibition of production of bisphenol A and several of their analogs in some countries.

Cyclodextrins (CD) are cyclic oligosaccharides composed of 6(α-CD), 7(β-CD) or 8(γ-CD) residuals of α-D-glucopyranose molecules joined in macrocycles by α-D-1,4 glycosidic linkages. Such structure ensures the presence of an inner hydrophobic cavity and an external hydrophilic periphery which allows them to form “host-guest” inclusion complexes with various hydrophobic molecules [7]. Such complexation often leads to significant changes in the “guest” molecule photochemistry and photophysics and to an increase of the “guest” photodegradation in particular. As bisphenols exhibit rather intensive absorption bands in UV region both direct and CD-assisted photolysis of bisphenols could be one of possible technique of water purification among other (bio)chemical and catalytic approaches [8].

It was found recently that DPA forms stable 1:1 inclusion complex with β-CD ($K_{st} = 6 \times 10^4\ M^{-1}$) and such complexation leads to great increase of UV degradation of the bisphenol [9]. This work is devoted to investigation of photophysics and photochemistry of DPA and DPA-βCD complex by means of nanosecond laser flash photolysis and picosecond fluorescence methods. Main attention is paid to determination of nature, spectral and kinetic properties of excited states and primary intermediates as well as clarification of mechanism of DPA photodegradation enhancement upon complexation with β-CD.

2. Materials and methods

A set-up for laser flash photolysis which utilizes forth harmonic (266 nm) of a Nd:YAG laser (LS-2137U, Solar, Belarus) as an

---

* Corresponding author. Tel.: +7 383 3332385; fax: +7 383 3307350.
E-mail addresses: salomatova@kinetics.nsc.ru (V.A. Salomatova), valen@tomo.nsc.ru (V.V. Yanshole), fengwu@whu.edu.cn (F. Wu).

1010-6030/$ – see front matter © 2013 Elsevier B.V. All rights reserved.
http://dx.doi.org/10.1016/j.jphotochem.2013.09.013

excitation source (pulse duration 6 ns, pulse energy 0.5–12 mJ/pulse) [10] was used in the experiments. Time resolution of the set up was 50 ns. For calculation of quantum yields (mean errors ±20%), laser intensity were measured by means of SOLO 2 laser power meter (Gentec EO). For monitoring the transient absorption changes in millisecond time domain the stationary diode (λ = 400 nm, 1 mW) was used as a probing light source.

UV absorption spectra were recorded using an Agilent 8453 spectrophotometer (Agilent Technologies). The fluorescence spectra and kinetics were measured on a FLSP920 spectrofluorimeter (Edinburg Instrument). As excitation sources ozone free xenon lamp Xe900 (λ_{ex} = 270 nm) and laser diode EPLED-280 (λ_{ex} = 280 nm, pulse duration of 800 ps) were used, correspondingly. The fluorescence quantum yields of DPA and DPA-βCD complex were determined as described in [11] using solutions of tryptophan in water (ϕ = 0.14) as a standard. Kinetic curves were fitted by iterative reconvolution of one or two exponential functions with the instrument response function, which allows to determine fluorescence life-times as short as 50 ps.

LCMS experiments were performed using ESI ion trap mass-spectrometer Esquire 6000 (Bruker Daltonics) with the HPLC-separation system Agilent 1200 Series. Separation was performed on an analytical column Zorbax SB300-C8, 1.0 mm × 150 mm, 3.5 μm in the gradient ACN/0.1% formic acid: 2% (0–5 min), 2–40% (5–10 min), 40–95% (10–37 min), 95% (37–43 min), 95–2% (43–44 min), 2% (44–55 min); flow rate 50 μl/min, sample volume 8 μl. Experimental parameters: registration of ions in negative mode, range 50–1000 m/z, HV capillary 4000 V, end plate offset −500 V, ESI nebulizer pressure 20 psi, dry gas flow (N_2) 10 l/min, temperature 300 °C.

HPLC experiments were performed using the Agilent LC 1200 chromatograph with diode array detector. Separation was performed on an analytical column Zorbax Eclipse XBD-C18 4.6 mm × 150 mm in the gradient ACN/0.05% trifluoroacetic acid: 0% (0–5 min), 0–50% (5–45 min), 50–100% (45–50 min), 100% (50–55 min) 100–0% (55–55.1 min), 0% (55.1–65 min); flow rate was 0.5 ml/min. Registration of chromatogram (260, 280, 320 and 400 nm) and peak area integration was done by software package Agilent ChemStation.

DPA ("Aldrich", 98%) and β-CD ("Wako Pure Chemical Inc.", >97%) (Fig. 1), acetonitrile (ACN, "Cryochrom", quality "0") and butylacetate (BuOAc, LC grade) were used without further purification. Typical concentrations of reagents in photochemical experiments were 3.6×10^{-4} and 1.5×10^{-3} M for DPA and β-CD, accordingly. In these conditions main part of DPA is bound in 1:1 complex with β-CD ($K_{st} = 6 \times 10^4\ M^{-1}$ [9]).

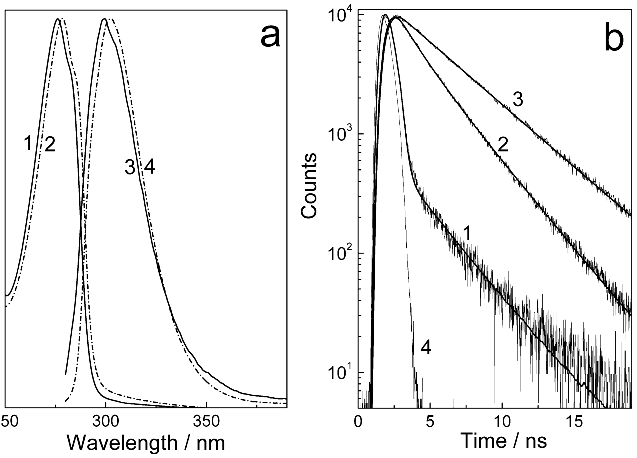

Fig. 2. (a) Normalized absorption (1, 2) and fluorescence (3, 4) spectra of DPA (1, 3) and DPA-βCD (2, 4) complex. (b) Kinetic curves of fluorescence at 310 nm for DPA in water (1), DPA-βCD in water (2), DPA in ACN (3) and the instrument response function (4). Smooth lines are the best mono and biexponential fit after reconvolution with the instrument response function. The second very weak component (1.5% of amplitude) at curve (1) corresponds to fluorescence of an impurity in DPA.

Unless otherwise stated, all experiments were run in a fused-silica cell with an optical path length of 1 cm at room temperature and atmospheric pressure in argon- or oxygen-saturated ($[O_2] = 1.4 \times 10^{-3}$ mol/l [12]) aqueous solutions. Double distilled or deionized water was used in all experiments.

3. Results and discussion

3.1. Spectroscopy of DPA and DPA-βCD complex

Optical and fluorescence spectra of the DPA-βCD complex and DPA are shown in Fig. 2a and the fluorescence decay curves in Fig. 2b. Complexation of DPA with β-CD leads only to a small red shift of the long-wavelength absorption band (π–π transition) (Table 1) and practically does not change the shape of the fluorescence band. However, drastic increase of fluorescence quantum yield and lifetime was observed upon complexation of DPA with β-CD (Table 1). This fact could be explained by restricted mobility of DPA in β-CD cavity leading to sharp decrease of the rate of internal conversion in the excited state, by shielding of this state from water molecules or by changing of the local polarity of media [13–15].

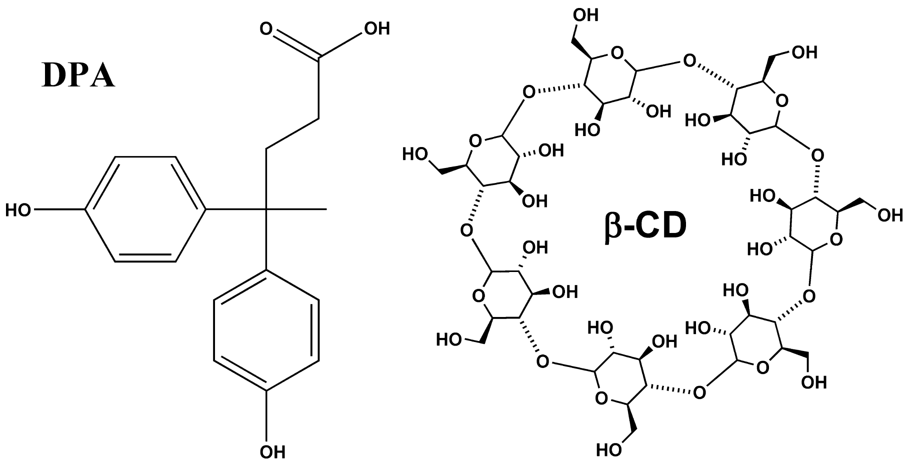

Fig. 1. Structural formulae of 4,4-Bis(4-hydroxyphenyl)valeric acid and β-cyclodextrin.

Table 1
Photochemical and photophysical properties of DPA and DPA-βCD.

	DPA in H_2O	DPA-βCD in H_2O	DPA in ACN	DPA in BuOAc
λ_{max}^{abs}/nm	276	279	279	279
λ_{max}^{fl}/nm	300	303	301	301
ε_{max}/M^{-1} cm^{-1}	3000	3200	–	–
ϕ_{fl}	0.01	0.14	0.23	0.06
τ_{fl}/ns	0.17	2.9	4.1	0.91

In order to distinguish between these possibilities the fluorescent measurements were carried out in ACN and BuOAc. First solvent has a high polarity close to water ($\varepsilon = 38$) but cannot form hydrogen bonds and cannot quench the excited states of molecules by proton transfer. Second solvent has a low polarity ($\varepsilon = 4.9$) and can form hydrogen bonds, which allows to check influence of these two parameters on lifetime of DPA excited state.

Both fluorescence quantum yield and lifetime of DPA are much higher in ACN than in water and BuOAc (Table 1) allowing one to conclude that protection of included DPA by β-CD from quenching by the solvent is the main reason of elongation of DPA fluorescence lifetime in the complex.

For close analogs of DPA studied in works [9,16–18] the structure of inclusion complex in which one of phenol rings of bisphenol is immersed in CD cavity and another is in the bulk solvent was proposed. Also, in works [9,16–18] Benesi Hildebrand equation was used to determine stochiometry of β-CD complexes with bisphenols. In all cases stochiometry was found to be 1:1 including for DPA-βCD complex [9]. Determination of exact structure of DPA-βCD complex is out of scope of current paper and will be a subject of further studies by means of NMR spectroscopy.

3.2. *Laser flash photolysis of DPA and DPA-βCD complex*

Flash excitation of the oxygen-free aqueous solutions of DPA (266 nm) gives rise to intermediate absorption consisting of the bands with maxima at 400 and 720 nm (Fig. 3a). These bands decay at substantially different rates (Fig. 3a), which indicate the formation of two intermediate species after the laser pulse. Based on the data on the pulse radiolysis, it is known that a wide band with a maximum at 720 nm belongs to the absorption of a hydrated electron (e_{aq}^-, $\varepsilon^{720} = 2.27 \times 10^4$ M^{-1} cm^{-1}) [20,21]. Thus, UV excitation of DPA leads to photoionization with formation hydrated electron–phenoxyl radical ($ArO^\bullet$) pair which is typical behavior for phenols and bisphenols in aqueous solution [19,22]. No evidence of DPA triplet state formation was obtained due to either very low quantum yield of this state or its absorption in far UV region (<300 nm) unavailable for registration by the flash photolysis setup. The last variant seems to be more probable as triplet state of unsubstituted phenol exhibits maximum of absorption at 260 nm [23].

In oxygen-saturated solutions the hydrated electron decays very rapidly in reaction with dissolved oxygen forming low-absorbing in UV region superoxide radical-anion ($k = 2 \times 10^{10}$ M^{-1} s^{-1} [20]). This fact allows to record the absorption spectrum of the $ArO^\bullet$ radical resulting from DPA photoionization (Fig. 3a, insert). The spectrum of $ArO^\bullet$ consists of three absorption bands with maxima at ≈300, 400 and ≈530 nm and coincides very well with known spectra of phenoxyl radicals of biphenols [24,25].

UV excitation of DPA-βCD complex also leads to photoionization of the bisphenol (Fig. 3b). Absorption spectrum of $ArO^\bullet$ in the β-CD cavity ($ArO^\bullet$-βCD) is close to the spectrum of $ArO^\bullet$ in solution (Fig. 3b, insert).

The yields of both hydrated electron and $ArO^\bullet$ radical exhibit non-linear dependence upon laser pulse energy (Fig. 4a) indicating that at high excitation intensity both monophotonic and biphotonic ionization of DPA takes place.

The best fit of the experimental data by the second order polynomial dependence ($\Delta A = a \times I + b \times I^2$) allows one to estimate the quantum yield of DPA monophotonic photoionization, $\phi(266\,nm) \approx 10^{-2}$. Absorption coefficient of $ArO^\bullet$ ($\varepsilon^{400} = 3.2 \times 10^3$ M^{-1} cm^{-1}) was determined by measuring the magnitude of the radical absorption at 400 nm (ΔA^{400}) (flash photolysis of DPA in oxygen-saturated solutions) and the concentration of hydrated electrons (flash photolysis of DPA in argon-saturated solutions) at various intensities of the excitation laser pulse

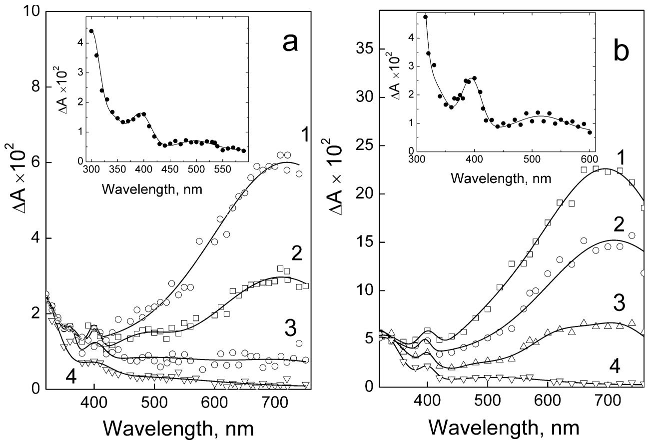

Fig. 3. (a) Transient absorption spectra recorded 0.05 μs (1), 0.4 μs (2), 1.2 μs (3) and 20 μs (4) after the laser excitation of DPA in argon-saturated aqueous solution. Insert – absorption spectrum of $ArO^\bullet$ radical recorded 1.6 μs after the laser excitation of DPA in oxygen-saturated aqueous solution. (b) Transient absorption spectra recorded 0.05 μs (1), 0.4 μs (2), 1.2 μs (3) and 20 μs (4) after the laser excitation of DPA-βCD in argon-saturated aqueous solution. Insert – absorption spectrum of $ArO^\bullet$-βCD radical recorded 0.8 μs after the laser excitation of DPA-βCD in oxygen-saturated aqueous solution.

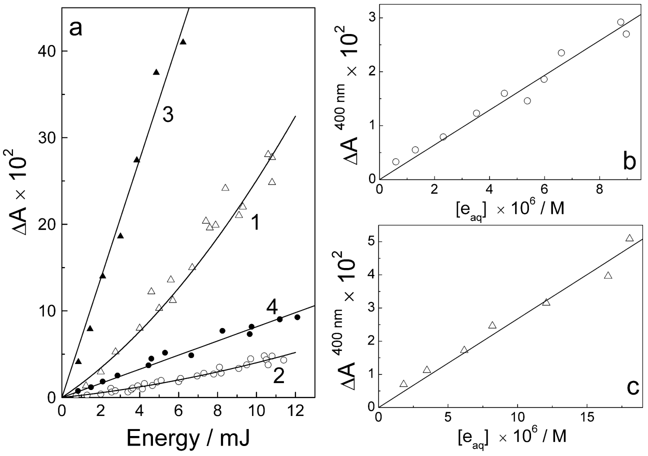

Fig. 4. (a) The dependence of the yields of hydrated electron (1, 3) and $ArO^\bullet$ radical (2, 4) from laser pulse energy upon photolysis of DPA (1, 2) and DPA-βCD (3, 4). Smooth lines are the best second order polynomial fit ($\Delta A = a \times I + b \times I^2$). (b and c) – Dependence of ΔA^{400} on the initial concentration of a hydrated electron upon photolysis of DPA (b) and DPA-βCD (c).

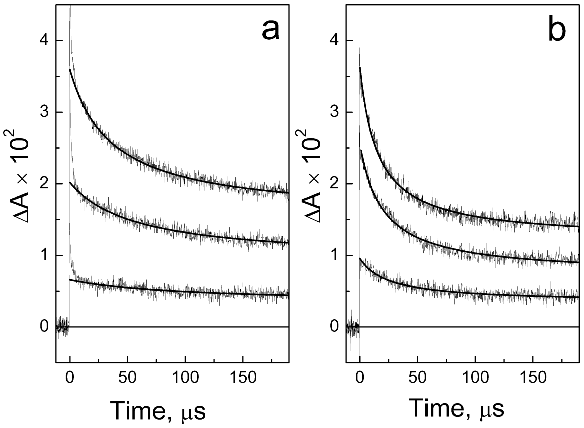

Fig. 5. Flash photolysis of DPA-βCD complex. Kinetic curves at 400 nm in oxygen-free (a) and oxygen-saturated (b) aqueous solutions at different excitation energy. Smooth curves are the best fit by formula (3). Initial fast part of kinetic curves at (a) is assigned to hydrated electron decay.

(Fig. 4b). This value is in a good agreement with known values of absorption coefficients of phenoxyl radicals [24,25].

The yields of both hydrated electron and ArO•-βCD radical formed by the photolysis of DPA-βCD complex exhibit good linear dependence upon laser pulse energy (Fig. 4a) indicating that mainly monophotonic ionization takes place in the energy region used. Photoionization quantum yield in monophotonic process in the case of the complex (ϕ(266 nm) = 4.1 × 10^{-2}) is four times higher than in case of DPA due to elongation of lifetime of the excited state of DPA in the inclusion complex. Absorption coefficient of ArO•-βCD ($\varepsilon^{400} = 2.8 \times 10^3\ \mathrm{M^{-1}\,cm^{-1}}$) was determined by the method described earlier for ArO• (Fig. 4c) and in the range of experimental error is the same as for phenoxyl radical in solution.

Phenoxyl radicals could decay in the recombination reaction yielding dimeric products (dihydroxybiphenyls) or the disproportion to give the parent compound and the corresponding quinine [26,27]:

$$\mathrm{ArO^\bullet + ArO^\bullet \rightarrow products} \qquad (1)$$

Also phenoxyl radicals could react with superoxide anion-radical with generation of corresponding peroxy-anion [27]:

$$\mathrm{ArO^\bullet + O_2{}^{-\bullet} \rightarrow ArOO_2{}^-} \qquad (2)$$

Indeed, decay of ArO• radicals in oxygen-free (Fig. 5a) as well as in oxygen-saturated (Fig. 5b) solutions are well described by second order low. Magnitude of transient absorption reaches an approximately constant value at time about 200 μs which indicates to the formation of long-lived photoproduct(-s). It worth to note that kinetic curves at 400 nm are identical in both air- and oxygen-saturated solutions indicating the absence of ArO• reaction with oxygen. This coincides well with low reactivity of phenoxyl radicals toward oxygen [28].

For aqueous solution of DPA without and in presence β-CD the kinetic curves of transient absorption decay at 400 nm in microsecond time domain are well described by formula (3):

$$\Delta A(t) = \frac{\Delta A_0 + \Delta A_p k_{obs} t}{1 + k_{obs} t} \qquad (3)$$

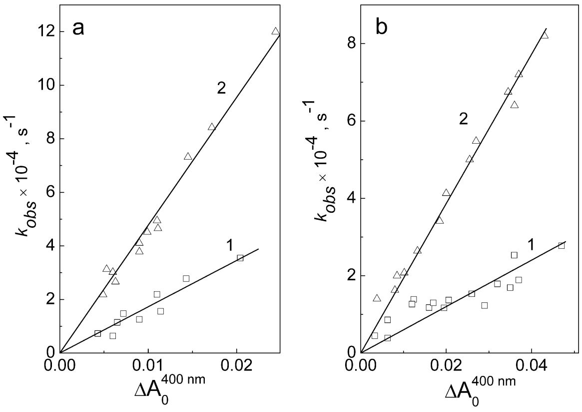

Fig. 6. Dependence of observed second-order rate constant of ArO• decay (k_{obs}) from initial absorbance at 400 nm (ΔA_0^{400}) for DPA (a) and DPA-βCD (b) in oxygen-free (1) and oxygen-saturated (2) aqueous solutions.

where ΔA_0 – initial amplitude of ArO• absorption at 400 nm, ΔA_p – absorption connected with accumulation of long-lived photoproduct(-s); k_{obs} – observed second-order rate constant of ArO• radical decay.

In oxygen-free solutions k_{obs} should be the linear function of ΔA_0^{400}:

$$k_{obs} = \frac{2k_1}{\varepsilon_{ArO}} \Delta A_0$$

where ε_{ArO} – the absorption coefficient of ArO• radical at 400 nm, k_1 – the rate constant of reaction (1). In oxygen-saturated solutions formula (3) is not exact and could be used only as simple and rough approximation of real complex decay of ArO• radicals. In the last case k_{obs} will be roughly expressed as following:

$$k_{obs} = \frac{2k_1 + k_2}{\varepsilon_{ArO}} \Delta A_0$$

where k_2 – the rate constant of reaction (2).

Indeed, the treatment of the set of kinetic curves at 400 nm at different ArO• concentration (Fig. 5a and b) by formula (3) gives a good linear dependence of k_{obs} from ΔA_0^{400} (Fig. 6a and b) in both oxygen-free and oxygen-saturated solutions which allows to estimates the rate constants of ArO• bimolecular decay in reactions (1) and (2) (Table 2). Values of k_{obs} are roughly 3 times higher in oxygen-saturated solution indicating big contribution of reaction (2) in the decay of the phenoxyl radicals. Decrease of $2k_1$ for ArO• situated in β-CD cavity is connected most probably with decreasing of diffusion mobility of the radical in the inclusion complex.

It worth to note that yield of long-lived absorption at 400 nm depends linearly from initial concentration ArO• radicals, does not depend on presence of β-CD in solution and decrease slightly in presence of dissolved oxygen (Table 2). All these findings allow to conclude that main channel responsible for long-lived absorption formation is the reaction (1).

In millisecond time domain for both DPA and DPA-βCD systems the fast initial decrease of optical density connected with decay of ArO• radicals is observed (Fig. 7b). However, 200 μs after excitation of DPA additional slow decrease of optical density at 400 nm reaching constant value at ~2 ms is observed.

Table 2
Results of treatment of experimental kinetic curves at 400 nm for DPA and DPA-βCD complex in argon-saturated (Ar) and oxygen-saturated (O_2) solutions.

	$2k_1 \times 10^{-9}/\mathrm{M^{-1}\,s^{-1}}$ (Ar)	$(2k_1 + k_2) \times 10^{-9}/\mathrm{M^{-1}\,s^{-1}}$ (O_2)	$\Delta A_p/\Delta A_0$ (Ar)	$\Delta A_p/\Delta A_0$ (O_2)
DPA	5.4	15	0.37	0.29
DPA-βCD	1.7	5.4	0.33	0.3

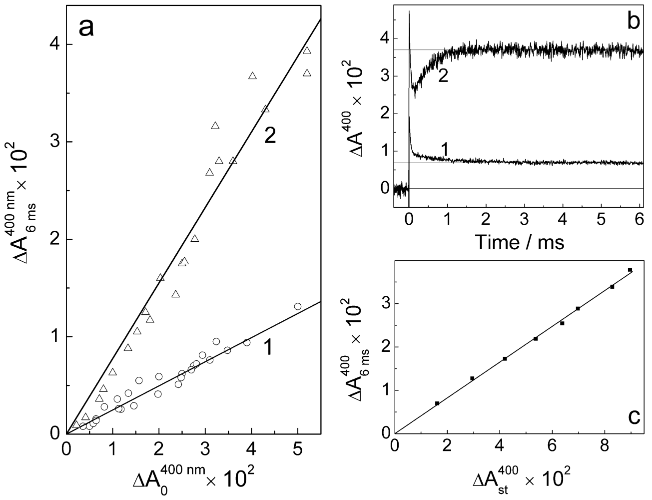

Fig. 7. (a) Dependence $\Delta A^{400}_{6\,\mathrm{ms}}$ at photolysis of DPA (1) and DPA-βCD (2) upon initial amplitude of ArO• absorption at 400 nm (ΔA^{400}_{0}); (b) kinetic curves at 400 nm in millisecond time range for DPA (1) and DPA-βCD (2). Excitation energy is 6.5 mJ. (c) Dependence $\Delta A^{400}_{6\,\mathrm{ms}}$ at photolysis of DPA-βCD upon stationary sample absorption at 400 nm ($\Delta A^{400}_{\mathrm{st}}$).

For DPA-βCD system in opposite additional increase of absorbance was detected which is also reached the constant value at times higher than 2 ms after laser flash (Fig. 7b). This data indicates formation in reaction (1) some unidentified transient product (possibly the diketo state which is primary product of two phenoxyl radical recombination) decaying in millisecond time range.

Parallel measurements by flash and stationary photolysis indicate that value of constant absorbance in millisecond scale ($\Delta A^{400}_{6\,\mathrm{ms}}$) for both systems depends linearly from ΔA^{400}_{0} (Fig. 7a) as well as from stationary absorbance of final photoproducts at 400 nm measured spectrophotometrically (Figs. 7c and 8a). The slope of the last dependence (Fig. 7c) well coincides with the ratio of irradiated volume to the total one. So one can conclude that the long-lived absorption in millisecond time range belongs to final photoproduct(-s) of phenoxyl radical reactions.

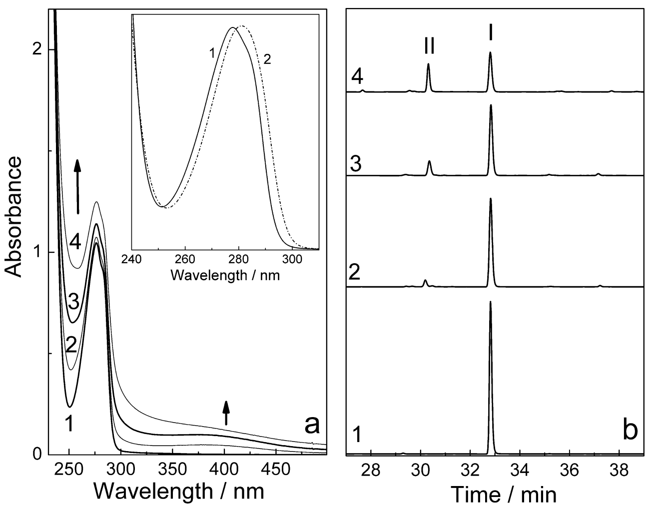

Fig. 8. Optical spectra (a) and chromatograms at 280 nm (b) of irradiated air-saturated DPA aqueous solution after 0 (1), 400 (2), 900 (3) 1900 (4) laser pulses (6.5 mJ/pulses). Peak (I) belongs to DPA, peak (II) – to the main photoproduct, hydroxylated DPA. Insert on (a) shows normalized absorption spectra of DPA (1) and main photoproduct (2).

Table 3
Results of LC–MS analysis of irradiated DPA.

Retention time/min	m/z	Possible structure
13.2	301.0	Hydroxylated DPA (Fig. 9)
13.8	285.0	DPA
15.4	569.1	C—C dimer (Fig. 9)

3.3. Stationary photolysis of DPA and DPA-βCD complex and photoproducts identification

Transformation of optical spectrum of air-saturated DPA solution during irradiation by flashes of Nd:YAG laser is shown on Fig. 8a, maximal absorption increase is observed at 245, 290 and 390 nm. As result of photolysis of both DPA and DPA-βCD single main photoproduct of higher polarity than DPA is formed (peak II), which optical spectrum is very close to the one of the initial compound (Fig. 8a and b). Analysis of the mass-spectrometric data (Table 3) leads to the conclusion that this product is hydroxylated DPA (m/z = 301.0 for photoproduct and 285.0 for DPA). These findings correspond to data concerning bisphenol E photochemistry [17]. One of the other minor products to be identified by mass spectrum is C—C dimer (m/z = 569.1), formed in reaction (1).

During the photolysis formation of many small peaks corresponding to minor photoproducts is also observed (Fig. 8b). These products are responsible for absorption increase at 245 and ≈400 nm during photolysis of DPA. Most probably that minor photoproducts have a quinoid nature because of intensive absorption at 245 nm is a characteristic feature of p-benzoquinone [29] and both o-quinones and diphenoquinones exhibit a good absorption at 400 nm [29,30]. This suggestion is supported by decreasing of yield of absorbance at 400 nm in stationary photolysis of DPA in oxygen-free solution. It worth to note that complexation with β-CD leads to increasing of the yield of photoproduct(-s) absorbing at 400 nm which is in agreement with flash photolysis data (Fig. 7b).

Calculated from LC data change of DPA concentration upon absorbed energy (Fig. 8b) allows to estimate quantum yield of DPA

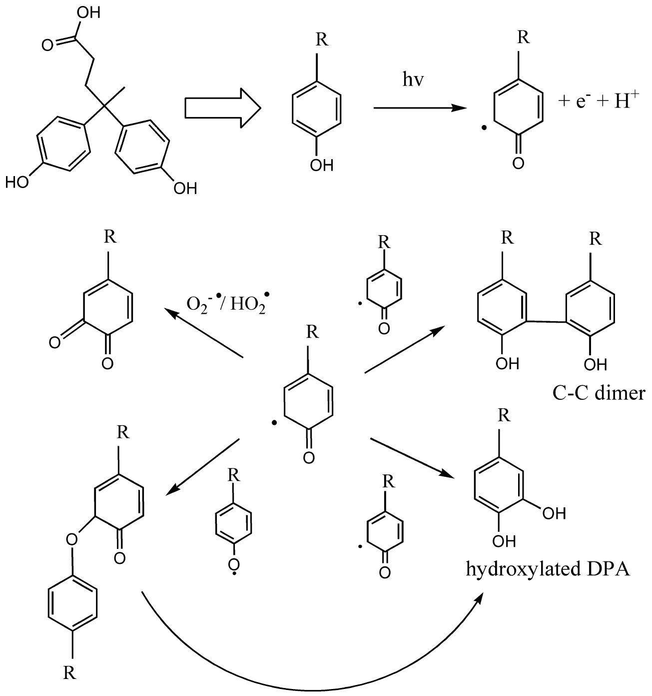

Fig. 9. Proposed scheme of DPA photolysis in the presence of oxygen.

photodegradation, $\varphi_{\text{degr}}(E_{\text{ex}} = 6\,\text{mJ}) = 0.036$. It worth to note that quantum yield of ionization at this energy is two times lower, $\varphi_{\text{ion}}(E_{\text{ex}} = 6\,\text{mJ}) = 0.017$. This fact could be explained by additional oxidation of DPA by superoxide anion-radical/hydrogen peroxide formed in the system:

$$\text{ArOH} + \text{O}_2{}^{-\bullet} + \text{H}^+ \rightarrow \text{ArO}^\bullet + \text{H}_2\text{O}_2$$

$$2\text{O}_2{}^{-\bullet} + 2\text{H}^+ \rightarrow \text{H}_2\text{O}_2 + \text{O}_2$$

$$\text{ArOH} + \text{H}_2\text{O}_2 \rightarrow \text{products} + 2\text{H}_2\text{O}$$

Transformation of optical spectra upon DPA-βCD photolysis is similar to the case of DPA, however photodegradation of the bisphenol in inclusion complex is more effective, $\varphi_{\text{degr}}(E_{\text{ex}} = 6\,\text{mJ}) = 0.11$. LC chromatography of DPA-βCD photolysed solution indicates on the formation of two main peaks, one of them is the same as for main photoproduct of DPA photolysis. More detailed analysis of photoproduct of DPA-βCD photolysis will be a subject of further work.

Analysis of the set of aforesaid kinetic and spectral data allows to proposed scheme of DPA and DPA-βCD photolysis in aqueous solutions (Fig. 9).

4. Conclusions

Photophysics and photochemistry of DPA and DPA-βCD inclusion complex were studied by laser flash photolysis, time-resolved fluorescence and LC methods. For both systems the photoionization with formation phenoxyl radical–hydrated electron pair is the main photochemical process. Complexation with β-CD leads to increase both photoionization and photodegradation quantum yields of the bisphenol connected with increase of excited state lifetime of DPA in the cyclodextrin cavity. In presence of oxygen phenoxyl radical decays in self-reactions and reaction with superoxide anion-radical with formation of long-lived transient product. The latter decays in millisecond time scale giving final photochemical products (hydroxylated DPA mainly).

Acknowledgments

The work was financially supported by the Federal target program “Scientific and scientific-pedagogical staff of innovative Russia” 2009–2013, SK No. 8175, the Russian Foundation for Fundamental Research (grants 11-03-00268, 12-03-00482, 12-03-91153-GFEN) and NSFC-RFBR grants (21211120159 and 21281220200).

References

[1] Y.H. Guo, K.X. Li, J.H. Clark, The synthesis of diphenolic acid using the periodic mesoporous $H_3PW_{12}O_{40}$-silica composite catalysed reaction of levulinic acid, Green Chem. 9 (2007) 839–841.

[2] M.-Y. Chen, M. Ike, M. Fujita, Acute toxicity, mutagenicity, and estrogenicity of bisphenol-A and other bisphenols, Environ. Toxicol. 17 (2002) 80–86.

[3] S. Kitamura, T. Suzuki, S. Sanoh, R. Kohta, N. Jinno, K. Sugihara, S. Yoshihara, N. Fujimoto, H. Watanabe, S. Ohta, Comparative study of the endocrine-disrupting activity of bisphenol A and 19 related compounds, Toxicol. Sci. 84 (2005) 249–259.

[4] A. Atkinson, D. Roy, In vitro conversion of environmental estrogenic chemical bisphenol A to DNA binding metabolites, Biochem. Biophys. Res. Commun. 210 (1995) 424–433.

[5] N. Cabaton, D. Zalko, E. Rathahao, C. Canlet, G. Delous, M. Chagnon, J. Cravedi, E. Perdu, Biotransformation of bisphenol F by human and rat liver subcellular fractions, Toxicol. In Vitro 22 (2008) 1697–1704.

[6] P. Chen, K. Linden, D. Hinton, S. Kashiwada, E. Rosenfeldt, S. Kullman, Biological assessment of bisphenol A degradation in water following direct photolysis and UV advanced oxidation, Chemosphere 65 (2006) 1094–1102.

[7] A. Douhal, Cyclodextrin Materials: Photochemistry, Photophysics and Photobiology, Elsevier, Amsterdam, 2006.

[8] E.J. Rosenfeld, K.G. Linden, Degradation of endocrine disrupting chemicals bisphenol A, ethinyl estradiol, and estradiol during UV photolysis and advanced oxidation processes, Environ. Sci. Technol. 38 (2004) 5476–5483.

[9] L. Guo, B. Wang, W. Huang, F. Wu, J. Huang, Photocatalytic Degradation of Diphenolic Acid in the Presence of β-Cyclodextrin Under UV Light, in: Book of Abstract of International Conference on Environmental Science and Information Application Technology, vol. 3, 2009, pp. 322–324.

[10] I.P. Pozdnyakov, V.F. Plyusnin, V.P. Grivin, D.Yu. Vorobyev, N.M. Bazhin, S. Pages, E. Vauthey, Photolysis of sulfosalicylic acid in aqueous solutions over a wide pH range, J. Photochem. Photobiol. A: Chem. 181 (2006) 37.

[11] D.F. Eaton, Reference materials for fluorescence measurement, Pure Appl. Chem. 60 (1988) 1107.

[12] R. Battino, T.R. Rettich, T. Tominaga, The solubility of oxygen and ozone in liquids, J. Phys. Chem. Ref. Data 12 (1983) 163–178.

[13] A. Coly, J.-J. Aaron, Cyclodextrin-enhanced fluorescence and photochemically-induced fluorescence determination of five aromatic pesticides in water, Anal. Chim. Acta 360 (1998) 129–141.

[14] R.E. Galian, A.V. Veglia, R.H. Rossi, Cyclodextrin enhanced fluorimetric method for the determination of tryptamine, Analyst 123 (1998) 1587–1591.

[15] I.V. Enoch Vijayan Muthu, M. Swaminathan, Inclusion complexation of 2-amino-7-bromofluorene by β-cyclodextrin: spectral characteristics and the effect of pH, J. Fluoresc. 14 (2004) 751–756.

[16] G. Wang, F. Wu, X. Zhang, M. Luo, N. Deng, Enhanced photodegradation of bisphenol A in the presence of β-cyclodextrin under UV light, J. Chem. Technol. Biotechnol. 81 (2006) 805–811.

[17] G. Wang, X. Xue, H. Li, F. Wu, N. Deng, β-Cyclodextrin-enhanced photodegradation of bis(4-hydroxyphenyl)ethane under UV irradiation, J. Mol. Catal. A: Chem. 276 (2007) 143.

[18] G. Wang, F. Wu, X. Zhang, M. Luo, N. Deng, Enhanced photocatalytic degradation of bisphenol F by β-cyclodextrin in aqueous TiO_2 dispersion, Fresen. Environ. Bull. 15 (2006) 61–67.

[19] I.P. Pozdnyakov, L. Guo, E.M. Glebov, F. Wu, V.P. Grivin, V.F. Plyusnin, N. Deng, Aqueous photochemistry of bisphenol E in the presence of β-cyclodextrin, High Energy Chem. 45 (2011) 214–221.

[20] G.V. Buxton, C.L. Greenstock, W.P. Helman, A.B. Ross, Critical review of rate constants for reactions of hydrated electrons, hydrogen atoms and hydroxyl radicals, J. Phys. Chem. Ref. Data 17 (1998) 513–531.

[21] P.M. Hare, E.A. Price, D.M. Bartels, Hydrated electron extinction coefficient revisited, J. Phys. Chem. A 112 (2008) 6800–6802.

[22] C. Richard, G. Grabner, Mechanism of phototransformation of phenol and its derivatives in aqueous solution, in: P. Boule (Ed.), Handbook of Environmental Chemistry, vol. 2. Part L: Reactions and Processes: Environmental Photochemistry, Springer-Verlag, Berlin, 1999, pp. 217–241.

[23] D.V. Bent, E. Hayon, Excited states in chemistry of aromatic amino acids and related peptides: I. Tyrosine, J. Am. Chem. Soc. 97 (1975) 2599–2606.

[24] D.-Y. Dou, Y.-B. Liu, H.-W. Zhao, L. Kong, S.-D. Yao, Radiolysis and photolysis studies on active transient species of diethylstilbestrol, J. Photochem. Photobiol. A: Chem. 171 (2005) 209–214.

[25] M. Sarakha, M. Bolte, H.D. Burrows, The photo-oxidation of 2,6-dimethylphenol and monophenylphenols by uranyl ion in aqueous solution, J. Photochem. Photobiol. A: Chem. 107 (1997) 101–106.

[26] H.-J. Joschek, S.I. Miller, Photooxidation of phenol, cresols, and dihydroxybenzenes, J. Am. Chem. Soc. 88 (1966) 3273–3281.

[27] M. Ye, R.H. Schuler, Second-order combination reactions of phenoxyl radicals, J. Phys. Chem. 93 (1989) 1898–1902.

[28] P. Neta, J. Grodkowski, Constants for reactions of phenoxyl radicals in solution, J. Phys. Chem. Ref. Data 34 (2005) 109–199.

[29] A.M. Al-Ajlouni, A. Bakac, J.H. Espenson, Kinetics and mechanism of the oxidation of phenols by the oxochromium(IV) ion, Inorg. Chem. 32 (1993) 5792–5796.

[30] G. Albarran, W. Boggess, V. Rassolov, R.H. Schuler, Absorption spectrum, mass spectrometric properties, and electronic structure of 1,2-benzoquinone, J. Phys. Chem. A 114 (2010) 7470–7478.